

Instantaneous Response and Quantum Geometry of Insulators

Nishchhal Verma

Department of Physics, Columbia University, New York, NY 10027, USA

Raquel Queiroz*

*Department of Physics, Columbia University, New York, NY 10027, USA and
Center for Computational Quantum Physics, Flatiron Institute, New York, New York 10010, USA*

We present the time-dependent Quantum Geometric Tensor (tQGT) as a comprehensive tool for capturing the geometric character of insulators observable within linear response. We show that tQGT describes the zero-point motion of bound electrons and acts as a generating function for generalized sum rules of electronic conductivity. Therefore, tQGT enables a systematic and basis-independent framework to compute the instantaneous response of insulators, including optical mass, orbital angular momentum, and the dielectric constant in low-energy effective theories. It allows for a consistent approximation across these quantities upon restricting the number of occupied and unoccupied states in an effective low-energy description of an infinite quantum system. We outline how quantum geometry can be generated in periodic systems by lattice interference and examine spectral weight transfer from small frequencies to high frequencies by creating geometrically frustrated flat bands.

I. INTRODUCTION

In a groundbreaking result, Thouless *et.al.* proved that the quantization of Hall conductivity results from a topological invariant associated with the phase winding of the ground state wavefunction of an insulator [1]. It established for the first time that the linear response cannot be fully described by energy dispersion or charge density alone. Rather, the phases of the wavefunctions are essential to fully capture transport of quantum materials. Over the past decades, examining topological invariants imprinted in the phases of wavefunctions has become commonplace, and their significance for the physical properties of materials is now well appreciated [2–7].

The ubiquity of geometric contributions in linear [8, 9] (and nonlinear [10–12]) response is rooted in the fact that electromagnetic fields couple to materials via the bulk dipole moment and, as shown by King-Smith and Vanderbilt [13], the dipole moment is intimately tied to the Berry phases of the wavefunctions in insulators. Similar considerations have been shown to extend from orbital magnetic moment [14, 15] and electric permittivity [16] of insulators to superfluid stiffness [17, 18] and spectral weight [19–21] of superconductors. Non-linear responses are typically related to higher powers of the electric dipole operator and probe higher orders of geometry [22, 23].

Of particular interest to this work is the quantum geometric tensor, $\mathcal{Q} = g + i\Omega/2$, whose real and imaginary parts are the quantum metric (g) and Berry Curvature (Ω), respectively. While the Berry curvature accounts for the phase accumulated by a wavefunction following a closed path in parameter space [24], the quantum metric tracks the loss of norm or non-adiabaticity that occurs during the transformation [25, 26]. In real materials,

Berry curvature is limited by inversion and time reversal symmetry and often vanishes. The metric, on the other hand, is positive semi-definite and generally non-vanishing for both trivial and topological systems provided there is more than a single band. A pressing challenge is to identify a response that directly measures the quantum metric [27]. Though there has been progress [28–32], it is not a straightforward feat since typically the metric appears intertwined with energy pre-factors. These terms factor out only in certain limiting cases such as Landau levels or other flat bands [17, 33]. The only known exact statement that relates to the metric alone and is agnostic to band energies is given by the Souza-Wilkens-Martin (SWM) sum rule [34], which states that the first negative moment of the dynamical conductivity in insulators is exactly the quantum metric of the ground state [5].

More exact statements can be made for optical sum rules and their relation to quantum geometry for flat bands. A key example is the f -sum rule, which defines the plasma frequency and therefore also the effective mass of electronic systems. In certain flat-band superconductors, the f -sum rule includes the quantum geometry of the electronic bands [35]. Whether the relation between f -sum rule of superconductors is universally tied to quantum metric is an open question. Similarly, the correct expressions of the bulk orbital magnetic moment of an insulator and Berry curvature are very close but not the same [9, 14, 15, 36]. While it is apparent that all these cases *require* non-trivial quantum geometry, the exact relation between them is opaque. It is now too common to label any property affected by the wavefunctions as “quantum geometric” in origin, clearly hinting at the lack of a unifying principle, which urgently needs to be addressed.

In this work, we propose the time-dependent quantum mechanical zero-point motion of electrons as a unifying picture to consistently define the various geomet-

* raquel.queiroz@columbia.edu

ric properties of insulators within linear response. Motivated by the fact that quantum geometry is ultimately a consequence of projecting the position operator into the filled bands subspace [37, 38], we consider a time-dependent off-diagonal electric dipole operator $d = e\mathcal{D}$, with $\mathcal{D}(t) \equiv \hat{Q}\hat{r}_\mu(t)\hat{P}$ where \hat{P} is the projector into the ground state and $\hat{Q} = 1 - \hat{P}$ the complimentary projector. The dipole operator, which couples with both applied and background electromagnetic fields, induces transitions between occupied and unoccupied states which may be either virtual or in resonance if the field frequency matches the energy of the transition. Crucial to this picture is that with time, states evolve and accumulate phases in the matrix elements of the position operator. It is therefore natural to consider the the correlation function

$$\mathcal{Q}_{\mu\nu}(t-t') = \langle \mathcal{D}_\mu^\dagger(t)\mathcal{D}_\nu(t') \rangle = \text{tr} \left[\hat{P}r_\mu(t)\hat{Q}r_\nu(t') \right] \quad (1)$$

as the *time-dependent Quantum Geometric Tensor* (tQGT), first introduced in Ref. [16]. Intuitively, the tQGT tensor probes the spatial uncertainty in the position of an electron due to tunneling between two points in space via the virtual transitions. It is a completely quantum mechanical object, that reduces to the familiar quantum geometric tensor at $t = 0$ with quantum metric $g_{\mu\nu} = \text{Re}[\mathcal{Q}_{\mu\nu}(0)]$ and Berry curvature $\Omega_{\mu\nu} = 2\text{Im}[\mathcal{Q}_{\mu\nu}(0)]$. The tQGT is not Hermitian but can be separated into a Hermitian $\mathcal{Q}_{\mu\nu}(t) + \mathcal{Q}_{\nu\mu}(-t)$ and an anti-Hermitian ($\mathcal{Q}_{\mu\nu}(t) - \mathcal{Q}_{\nu\mu}(-t)$) part, of which the latter directly relates to the conductivity tensor.

The fact that dipole transitions lead to vacuum fluctuations is well known for isolated atoms interacting with a background gauge field [39]. The essence of our work is to extend this concept to infinite quantum systems in a gauge-independent fashion which can be straightforwardly computed given the energies and wavefunctions of a macroscopic insulator. By studying the zero point motion [40], we can unify the notion of quantum geometry with various physical quantities that relate, albeit indirectly, to quantum geometry, such as orbital magnetic moment, f -sum rule and dielectric permittivity. Importantly, we see that all these quantities cannot be independently approximated, and are all bound to a particular choice of occupied states \hat{P} and unoccupied states \hat{Q} in any low energy description. Moreover, tQGT provides a natural language to write generalized sum rules for the dissipative parts of optical conductivity, which have recently gained attention [41–44].

II. RESULTS

Our main results can be summarized in a rewriting of the Kubo formula for conductivity in terms of the time-dependent quantum geometric tensor in the time domain, and the consequent generalized form for the dissipative sum rules that tie various geometric properties of an in-

sulating system. To concisely isolate the dissipative response in conductivity, we define the axial vectors σ_μ^L and σ_λ^H to write the conductivity tensor as

$$\sigma_{\mu\nu} = \delta_{\mu\nu}\sigma_{L,\mu} + \epsilon_{\mu\nu\lambda}\sigma_{H,\lambda} \quad (2)$$

where μ, ν, λ are spatial indices and the superscripts L and H refer to Longitudinal and Hall responses (see App. E for details). Focusing on gapped quantum systems with charge conservation (see App. A), we write the conductivity in a spectral representation in terms of the matrix elements of the position operator

$$\sigma_{\mu\nu}(\omega) = -i\frac{e^2}{\hbar} \sum_{m \neq n} f_{nm}\omega_{nm}\hat{r}_\mu^{nm}\hat{r}_\nu^{mn} \frac{1}{\omega - \omega_{mn}} \quad (3)$$

where m, n are the energy states, $f_{nm} = f_n - f_m$ are the occupation factors with $\omega_{mn} = \omega_m - \omega_n$ being energy difference (see App. A for details). The formula points to generalized sum rules for the dissipative part of conductivity (see App. A 1 for details)

$$\mathcal{S}_{\mu\nu}^\eta = \int_0^\infty d\omega \frac{\sigma_{\mu\nu}^{\text{abs}}(\omega)}{\omega^{1-\eta}} = \delta_{\mu\nu}\mathcal{S}_{L,\mu} + i\epsilon_{\mu\nu\lambda}\mathcal{S}_{H,\lambda}. \quad (4)$$

The absorptive (or Hermitian) part is defined as $\sigma_{\mu\nu}^{\text{abs}} = (\sigma_{\mu\nu} + \sigma_{\nu\mu}^*)/2$ (see App. E for details). The half limit is crucial for differentiating the sum rule from standard Kramers-Kronig relations (see App. F). Notice that $\sigma_{\mu\nu}^{\text{abs}}(\omega)$ includes the real part of longitudinal conductivity $\text{Re}[\sigma_{L,\mu}(\omega)]$ and the imaginary part of Hall conductivity $\text{Im}[\sigma_{H,\lambda}(\omega)]$ [44]. Eq. (3) bears some similarities with the tQGT, which in the same representation is given by

$$\mathcal{Q}_{\mu\nu}(t-t') = \sum_{m \neq n} f_n(1-f_m)e^{i\omega_{mn}t} \hat{r}_{nm}^\mu \hat{r}_{mn}^\nu \quad (5)$$

If we choose to write the conductivity in the time domain (see App. B for details), we indeed find that it assumes a remarkably simple form

$$\sigma_{\mu\nu}(t) = \frac{\pi e^2}{\hbar} \Theta(t) \partial_t \mathcal{Q}_{\mu\nu}^{\text{as}}(t). \quad (6)$$

where $\mathcal{Q}_{\mu\nu}^{\text{as}}(t) = (\mathcal{Q}_{\mu\nu}(t) - \mathcal{Q}_{\nu\mu}(-t))/i$ is the anti-symmetric and anti-Hermitian part of the tQGT (see App. C for details). Note that Eq.(6) is valid for both metals and insulators, although in this work we focus on the latter, see a more detailed discussion in App. D. The relation between dynamics of electrons and conductivity is now evident, for insulators both $\mathcal{Q}_{\mu\nu}(t)$ and $\sigma_{\mu\nu}(t)$ have bounded oscillations that occur precisely because of the quantum geometry.

With this insight, it is straightforward to find an exact expression for all optical sum rules

$$\mathcal{S}_{L/H,\mu}^\eta = \frac{\pi e^2}{\hbar} \left[(-i\hat{\partial}_t)^\eta \mathcal{Q}_{L/H,\mu}(t) \right]_{t=0} \quad (7)$$

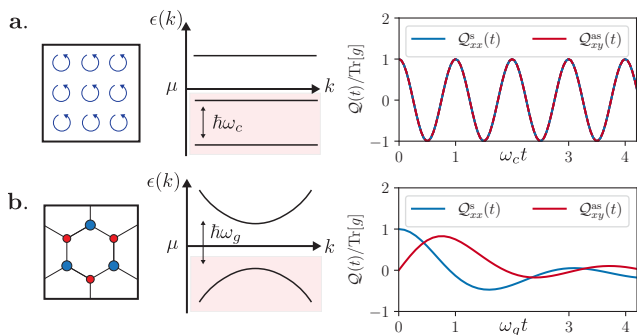


FIG. 1. **a.** Time-dependent quantum geometric tensor (tQGT) in Landau levels. The real longitudinal and imaginary Hall parts of the tQGT are identical and oscillate with the same frequency $\omega_c = \sqrt{eB/m}$. **b.** tQGT in a honeycomb lattice model with nearest neighbor hopping and a C_{2z} breaking mass term $m_z > 0$ (details in App. H1). Different parts of tQGT now have different time profiles. As a result, geometric quantities arising from different derivatives are all distinct.

where $\mathcal{Q}_{\mu\nu}(t)$ has been decomposed into longitudinal and Hall parts $\mathcal{Q}_{\mu\nu}(t) = \delta_{\mu\nu}\mathcal{Q}_{L,\mu}(t) + \epsilon_{\mu\nu\lambda}\mathcal{Q}_{H,\lambda}(t)$ for a succinct presentation. This is the main result of our work. Each sum rule (\mathcal{S}^η) can be associated with an instantaneous property characterizing the bound electrons of the insulator. This instantaneous response, given by the various derivatives of $\mathcal{Q}(t)$ at $t = 0$, defines various measurable properties associated with the zero-point motion of the bound charges. In particular, $\eta = 0$ is the SWM sum rule for insulators [34] and $\eta = 1$ is the f -sum rule that defines the plasma frequency $\omega_p^2 = 4\pi n e^2/m$ [45].

We begin by unpacking Eq. (7) for various η . The longitudinal and Hall sum rules take the explicit form

$$\mathcal{S}_{L,\mu}^\eta = \frac{\pi e^2}{\hbar} \sum_{\substack{n \in \text{filled} \\ m \in \text{empty}}} \omega_{mn}^\eta g_\mu^{nm}, \quad \mathcal{S}_{H,\lambda}^\eta = \frac{\pi e^2}{\hbar} \sum_{\substack{n \in \text{filled} \\ m \in \text{empty}}} \omega_{mn}^\eta \Omega_\lambda^{nm} \quad (8)$$

where $g_\mu^{nm} \equiv |\langle u_n | \hat{r}_\mu | u_m \rangle|^2$, $\Omega_\lambda^{nm} \equiv 2\text{Im}[\hat{\lambda} \cdot \langle u_n | \hat{\mathbf{r}} | u_m \rangle \times \langle u_m | \hat{\mathbf{r}} | u_n \rangle]$ are various matrix elements of the current operator and ω_{mn} is the energy difference between states $|u_m\rangle$ and $|u_n\rangle$. These matrix quantities are all gauge invariant under a $U(1)$ transformation that gives arbitrary phases to a band wavefunction for $m \neq n$. The case for $m = n$, which arises in metals, needs a more careful treatment that is outlined in App. D3.

The $\eta = 0$ sum rule has no energy prefactor. Its longitudinal part is the SWM sum rule and defines the quantum metric $\text{Tr}[g]$ where the trace is over occupied states, and its Hall part can be obtained from a Kramers-Kronig relation of the TKNN conductivity. It is simply the total Chern number \mathcal{C} of the system. The $\eta = 1$ sum rule defines the plasma frequency with $\omega_p^2 = 4\pi n e^2/m$ where n is the electron total density (including core electrons) and m is the bare mass of the electron, and from the Hall part one can read the orbital magnetic moment of insu-

lators as defined in Refs.[46, 47]. We should pause here to comment that in *ab-initio* calculations, which start with free electrons subjected to a periodic potential, the number of bands is infinite. The plasma frequency is independent of the periodic potential and the exact form of the wavefunctions and it is guaranteed to be $\propto n/m$ by the band mass theorem [48]. Deviations can occur for low-energy effective theories. For example, in a tight-binding model, especially those with multiple bands, the plasma frequency is renormalized [49, 50] and becomes sensitive to the wavefunctions [51]. Finally, the $\eta = -1$ sum rule defines the dielectric permittivity of the material [16]. Intuitively, it measures how much the electrons can polarize the medium in the presence of an electric field. The imaginary part of the same sum measures if electrons have a torsional twist in responding to an external electric field, reminiscent of the gyration vector [52].

The power of Eq. (8) lies in a consistent definition of the geometric properties of materials. The sum rules are not independent, and in fact become fixed once the projectors \hat{P} and \hat{Q} are fixed, as well as the band energies. Therefore, we present a consistent definition of instantaneous properties for effective tight-binding models obtained by selecting a subset of bands obtained by first principles. This subtlety has been especially relevant since the discovery of topological insulators. Topological indices act as an obstruction to finding a local basis that only has low-energy orbitals [53] while respecting all the spatial and internal symmetries [54, 55]. To describe topological phases with local Hamiltonians it is necessary to include multiple orbitals which mandates bounded oscillations in the tQGT.

To gain some familiarity with the tQGT, it is instructive to consider Landau levels in the two-dimensional electron gas as the simplest example of a topological insulator. In this case it takes the simple form with $\mathcal{Q}(t) = \mathcal{C}e^{i\omega_c t}$ where $\omega_c = \sqrt{eB/m}$ is cyclotron frequency and \mathcal{C} is the total Chern number. The sum rules can be immediately deduced

$$\mathcal{S}_{\mu\nu}^\eta = \mathcal{C}\omega_c^\eta (\delta_{\mu\nu} + i\epsilon_{\mu\nu z}) \quad (9)$$

where the area of the magnetic unit cell ($\ell_B^2 = eB/m$) cancels the volume normalization factor to give rise to the net Chern number \mathcal{C} . The precise analytical form of the Landau level wavefunction enforces quantum metric, Berry curvature, orbital magnetic moment, effective optical mass, and dielectric permittivity – all to be the same, up to factors of ω_c . This is consistent with the classical picture of electrons going around in cyclotron orbits in the plane perpendicular to the magnetic field. The challenge lies in extrapolating these concepts over to real materials that have non-flat dispersions and therefore non-trivial dynamics in the tQGT. Moreover, the wavefunctions themselves do not admit the so-called ideal band geometry [56, 57]. As a result, all the geometric quantities are different but related. Here, we find that sum rules allow us to straightforwardly compute these quantities.

III. MODEL AND METHODS

Optical conductivity is the static ($\mathbf{q} = 0$) response of a system to a dynamical ($\omega \neq 0$) field. The Kubo formula for conductivity in the exact many-body basis can be written formally as

$$\sigma_{\mu\nu}(\omega) = \frac{i}{\omega} (D_{\mu\nu} - \chi_{j_\mu, j_\nu}(\omega)) \quad (10)$$

where $D_{\mu\nu} \equiv \langle \partial_{A_\mu A_\nu} \mathcal{H}(A) \rangle - \text{Re}[\chi_{j,j}(0)]$ is the charge stiffness defined in terms of diamagnetic current and paramagnetic current-current correlator with $j_\mu \equiv \partial_{A_\mu} \mathcal{H}(A)$ [58]. The occupation factors are $f_{nm} = f_n - f_m$ with f_n being the occupation of state $|u_n\rangle$. The position matrix elements are $\hat{r}_\mu^{nm} \equiv \langle u_n | \hat{r}_\mu | u_m \rangle$ and $\omega_{nm} = \omega_n - \omega_m$ is the energy difference. The charge stiffness can be equivalently defined as the change in the ground state energy of the system following a twist in the boundary conditions [59]. It vanishes identically for a gapped quantum system with number conservation [60]. Considering such gapped quantum systems for now, we arrive at the Kubo formula for conductivity shown in Eq. (3). We focus on the dissipative component that arises from the imaginary part of $1/(\omega - \omega_{mn})$. In two dimensions, it corresponds to $\text{Re}[\sigma_{xx}]$ and $\text{Im}[\sigma_{xy}]$. The three dimensional generalization is straightforward with the axial representation $\Omega_{\mu\nu}^{mn} \equiv \epsilon_{\mu\nu\lambda} \Omega_\lambda^{mn}$ that is outlined in App. E. We rewrite absorptive part of the conductivity as

$$\sigma_{\mu\nu}^{\text{abs}}(\omega) = \delta_{\mu\nu} \text{Re}[\sigma_\mu^L] + i\epsilon_{\mu\nu\lambda} \text{Im}[\sigma_\lambda^H]. \quad (11)$$

The inclusion of the position operator in the Kubo formula is the key to extracting the quantum geometry. Consider the longitudinal part for instance

$$\text{Re}[\sigma_{L,x}(\omega)] = \frac{\pi e^2}{\hbar} \sum_{m \neq n} f_{nm} \omega_{nm} g_{L,\mu}^{nm} \delta(\omega - \omega_{mn}) \quad (12)$$

where the quantum metric is nearly present but the prefactor of ω_{mn} and the delta function prohibit g_{xx}^{nm} from becoming the quantum metric. One way to circumvent the issue is to consider sum rules that remove the delta function by the equality

$$\int_0^\infty d\omega \delta(\omega - \omega_{mn}) = \frac{\Theta(\omega_{mn})}{2}. \quad (13)$$

As we show next, different moments with $\omega^{\eta-1}$ then correspond to different geometric properties of the insulator, arising from the time-dependence of the zero point motion.

A. SWM Sum Rule and Quantum Geometry

The initial proposal behind the SWM sum rule [34] was aimed at classifying metallic and insulating states by

examining if $\text{Tr}[g]$ diverges in the thermodynamic limit [5], a line of reasoning that traces back to Kohn [59]. The value of $\text{Tr}[g]$ itself was not considered important provided it remained finite. However, with the refined classification of insulators [6] into atomic, obstructed, or topological, revisiting the sum rule has yielded significant new insights [41], applicable to both insulators [42] and narrow-gap semiconductors [43, 44].

In our notation, the sum rule takes the expression

$$\int_0^\infty d\omega \frac{\sigma_{\mu\nu}^{\text{abs}}(\omega)}{\omega} = \frac{\pi e^2}{\hbar} (\delta_{\mu\nu} \text{Tr}[g_{\mu\nu}] + i\epsilon_{\mu\nu\lambda} \mathcal{C}_\lambda) \quad (14)$$

whose real part is the SWM sum rule with $\text{Tr}[g_\mu]$ (trace over occupied states) and the imaginary part is the Chern number. We note that Chern number in $\text{Im}[\sigma_H(\omega)]$ sum rule is related to $\text{Re}[\sigma_\lambda^H(0)]$ as a consequence of Kramers–Kronig relations. As emphasized in Ref.[42], these sum rules quantify the quantum weight of insulators.

B. f -Sum Rule and Effective Mass

The f -sum rule is given by the real part of the longitudinal conductivity

$$\int_0^\infty d\omega \text{Re}[\sigma_{L,\mu}(\omega)] = \frac{\pi e^2}{\hbar} \sum_{\substack{n \in \text{filled} \\ m \in \text{empty}}} \omega_{mn} g_\mu^{nm} \quad (15)$$

and is used to define the plasma frequency ω_p^2 which involves the total electron density and bare electron mass.

In crystalline solids, the label for each quantum states breaks into band label m and crystal momentum label \mathbf{k} . As we outline in App. D, the algebra is identical except for the additional label and integral over \mathbf{k} . The plasma frequency in such systems is typically a large energy scale that includes all possible $\mathbf{q} = 0$ direct inter-band transitions that are allowed in $\text{Re}[\sigma_{L,\mu}]$.

The mass obtained from the sum rule deviates from the bare electron mass when we use low-energy sum rules that include transitions only between the low-energy orbitals. As the Hilbert space is truncated, for instance in tight-binding models, the band mass theorem no longer applies and the sum rule depends sensitively on wavefunctions. By requiring the low-energy plasma frequency to be proportional to n/m , we can define an effective mass for each filled band:

$$\mathcal{M}_{n,\mu}^{-1} \equiv \sum_{m \neq n} \omega_{mn} g_\mu^{mn}, \quad (16)$$

such that the sum rule is $\mathcal{S}_{L,\mu}^1 = \sum_{n \in \text{filled}} \mathcal{M}_{n,\mu}^{-1} \equiv n/m_g^*$ with m_g^* being the total geometric contribution to the effective mass. We emphasize that this is the only consistent way of defining optical mass in topological insulators.

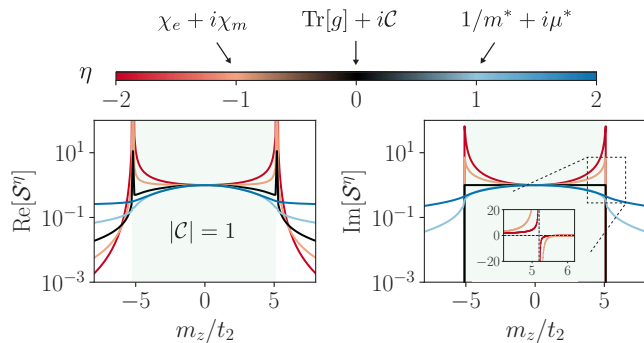


FIG. 2. Longitudinal and Hall sum rules ($S^\eta = S_L^\eta + iS_H^\eta$) for the two-dimensional Haldane Chern Insulator at half-filling across the topological phase transition that occurs at $|m_z/t_2| = 3\sqrt{3}$. The model includes a nearest neighbor hopping t , a next nearest neighbor hopping t_2 with flux $\phi = \pi/2$, and an inversion breaking mass m_z (see App. H 2 for details). The sum rules are normalized by their value at $m_z = 0$. The SWM sum rule (black) in the left panel corresponds to $\text{Tr}[g]$ and the Chern number \mathcal{C} . $\text{Tr}[g]$ diverges across the topological phase transition. The discontinuities become more smooth or divergent depending on the energy power η . Note that the Hall sum rules with $\eta \leq -1$ show an anti-symmetric divergence at the phase transition.

The theory extends easily to metals that are gapless and have a Fermi surface Drude contribution. As we show in App. D, the existence of Fermi-surface adds an unbounded linear-in-time contribution to the tQGT

$$\mathcal{Q}_{\mu\nu}(t) = D_{\mu\nu}t + \mathcal{Q}_{\mu\nu}^{\text{inter}}(t) + \dots \quad (17)$$

where (\dots) includes a time-independent piece that does not contribute to the f -sum rule (see App. D 2 for details). The Drude weight $D_{\mu\nu} = \sum_{n,\mathbf{k}} f_{n,\mathbf{k}} \partial_k^2 \epsilon_{n,\mathbf{k}}$ contributes only to the longitudinal conductivity. It adds a mass to the f -sum rule that is given by the band curvature, m_ϵ^* . In total, we get

$$\frac{1}{m^*} = \frac{1}{m_\epsilon^*} + \frac{1}{m_g^*} \quad (18)$$

such that the optical mass includes the geometric contribution and Fermi surface contributions in equal footing. It can be regarded as an effective band mass theorem for the low-energy states. Interactions modify the sum rule, however, within Fermi-liquid theory, the low-energy sum rule is tied to the Luttinger invariant [61, 62].

The geometric mass plays a crucial role in flat band superconductivity [18]. Without interactions, a flat band has an infinite density of states and a vanishing Fermi velocity. The band curvature is infinite, $1/m_\epsilon^* = 0$, but the geometric mass can still be finite. If the band is further isolated from the rest of the spectrum, the system is insulating and the associated tQGT has bounded oscillations. As the system becomes superconducting with an attractive Hubbard interaction U , the massively degenerate flat band manifold of states reorganizes into a

lower Hubbard band with doubly occupied sites and an upper Hubbard band with single occupancy [19]. With no single-particle bandwidth, the attractive interaction is the only energy scale in the problem. The low-energy effective theory then corresponds to bosons with hopping amplitude set by the interaction times the quantum metric [35, 63].

The strength of our definition in Eq. (1) is that it is agnostic to the ground state as long as it is gapped and the projector is well defined. It can be easily used to get an effective mass for the f -sum rule. As expected, it corresponds to n_b/m_b where n_b is the density of Cooper pairs and m_b the mass controlled by the boson hopping amplitude which is interaction times the quantum metric, $U \text{Tr}[g]$. The additional spectral weight has been verified numerically as well [64, 65].

The imaginary part of $\eta = 1$ sum rule is also interesting. It corresponds to the dichroic sum rule [66]

$$\int_0^\infty d\omega \text{Im}[\sigma_{H,\lambda}(\omega)] = \frac{\pi e^2}{\hbar} \sum_{\substack{n \in \text{filled} \\ m \in \text{empty}}} \omega_{mn} \Omega_\lambda^{nm} \quad (19)$$

and defines the bulk orbital magnetic moment of the system. This formula can be intuitively understood from a short time expansion of the tQGT in Eq. (1)

$$\mathcal{Q}_{\mu\nu}(t) \approx \mathcal{Q}_{\mu\nu}(0) + it \text{Tr}[\hat{P}[\hat{H}, \hat{r}_\mu] \hat{Q} \hat{r}_\nu] \quad (20)$$

where $[\hat{H}, \hat{r}_\mu] \equiv i\hbar \hat{v}_\mu$ is the velocity operator. The imaginary part of the first derivative then directly translates to an effective angular momentum $\approx \hat{z} \cdot \text{Tr}[\hat{P} \mathbf{v} \times \hat{Q} \mathbf{r}]$ from which the orbital magnetic moment can be derived [46].

C. Permittivity tensor

The $\eta = -1$ sum rule is defined only for insulators as

$$\int_0^\infty d\omega \frac{\sigma_{\mu\nu}^{\text{abs}}(\omega)}{\omega^2} = \frac{\pi e^2}{\hbar} (\chi_\mu^e \delta_{\mu\nu} + i\epsilon_{\mu\nu\lambda} \chi_\lambda^m) \quad (21)$$

where χ_μ^e defines the longitudinal polarizability of the material in response to an electric field. It relates to the longitudinal dielectric constant $\epsilon = 1 + \chi^e$, and the geometric capacitance $c = \epsilon_0 \chi^e$ [16] of an insulator. It quantifies the inverse spring constant of the electron that is tied to the atomic site. Here, ϵ_0 is the vacuum permittivity.

The Hall part of the sum rule, χ_λ^m , concerns imaginary part of the Hall conductivity $\text{Im}[\sigma_H(\omega)]$ which is itself related to the real part of the dielectric function $\text{Re}[\epsilon_H(\omega)]$. If the integral limits were taken from $-\infty$ to ∞ , the sum rule would evaluate to $\text{Re}[\epsilon_H(0)]$ (by Kramers-Kronig relation) and vanish identically. The sum rule survives because the limits are from 0 to ∞ . Now since it is no longer a Kramers-Kronig relation, the sum rule does not

correspond to an obvious zero-frequency property, similar to quantum metric $\text{Tr}[g]$ and magnetic moment μ_λ . Intuitively, $\text{Im}[\epsilon_H(\omega)]$ characterises absorption of circularly polarized light and appears in dichroic responses. Therefore, χ_λ^m is expected to capture the response of the electronic state to external fields of different polarization. Presumably it acts as a torsional constant, however, a precise definition is lacking.

D. Exact Bounds on Sum Rules

As we have emphasized in the previous section, different sum rules probe different instantaneous properties of the material. These properties are independent but have certain constraints which we now outline. Focusing on the longitudinal sum rule

$$\mathcal{S}_{L,\mu}^\eta = \int_0^\infty d\omega \frac{\text{Re}[\sigma_{L,\mu}(\omega)]}{\omega^{1-\eta}} \quad (22)$$

we find a series of exact bounds

$$\mathcal{S}_{L,\mu}^{m+n} \leq \sqrt{\mathcal{S}_{L,\mu}^{2m} \mathcal{S}_{L,\mu}^{2n}} \quad (23)$$

where m, n are arbitrary real numbers (see App. G for details). These bounds rely on the positive semi-definite property of $\text{Re}[\sigma_{L,\mu}]$ [67] and hence do not work for the imaginary parts. We also note that Landau levels trivially saturate the inequality. As seen in Eq. (9), all properties of Landau levels are one and the same upto factors of ω_c .

The bound is most insightful for $m = -n = -1/2$ where it yields $\mathcal{S}_{L,\mu}^0 \leq \sqrt{\mathcal{S}_{L,\mu}^1 \mathcal{S}_{L,\mu}^{-1}}$. In terms of material properties, it implies a universal inequality between quantum geometry, electric susceptibility and plasma frequency

$$\text{Tr}[g] \leq \omega_p \sqrt{\chi^e}. \quad (24)$$

The plasma frequency as written includes the bare mass of the electron and total density. It is a large number which can be modified, as outlined in the previous section, to get a tighter bound using a low-energy tight-binding description. However, we emphasize that all sum rules should be defined consistently following the same tQGT. In other words, they should all agree on the definition of the projector \hat{P} and \hat{Q} . This is important for computing bounds on a topological gap for instance [41].

Various sum rules are shown in Fig. 2 for the Haldane model of Chern insulator at half-filling across the topological transition. Interestingly, the Hall sum rules for $\eta \leq -1$ exhibit an anti-symmetric divergence near the transition.

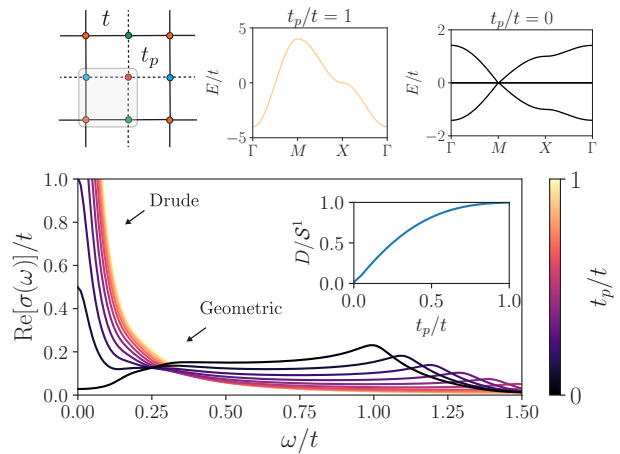


FIG. 3. Transfer of Spectral Weight to higher frequencies in the Lieb lattice model that interpolates to the square lattice with parameter t_p/t . At $t_p = t$, the square lattice has no geometric contribution and follows a Drude-like behavior. The inter-band transitions increase as t_p is reduced. Finally, at $t_p = 0$, one of the orbital factors out and the resulting Lieb lattice has a vanishing Drude weight. The optical conductivity, on the other hand, has a non-zero interband contribution coming from the minimal inter-band conductivity of a Dirac cone [68].

IV. INDUCING DYNAMICS IN TQGT

Two systems with identical spectrum can react differently to interactions due to difference in the wavefunctions. This variation is rooted in form factors that appear in projected interactions and can significantly influence the ground state of the system. In our language, this fact is imprinted in the bounded oscillations of $\mathcal{Q}(t)$. Understanding the origins of these oscillations, assessing their relevance, and determining when they might be negligible are some of the essential questions, particularly important in the context of moiré materials where flat bands emerge from an assembly of thousands of atoms [69]. In such materials, the nuanced effects of wavefunctions are expected to critically influence the correlated phenomena [70].

Let us investigate this effect in a simple toy model, where we illustrate the appearance of quantum geometry and oscillations in $\mathcal{Q}(t)$ with a single tuning parameter. We use a tight-binding model that interpolates between the Lieb lattice, which has a flat band, to the single band square lattice, which has no band geometry, by tuning t_p/t (see App. H3 for details). Here t is the hopping amplitude between nearest neighbors and t_p connects the plaquette orbital to the rest of the lattice, see Fig.3.

Initially, at $t_p = t$, the Hamiltonian is simply an electron in a square lattice at half filling and therefore exhibits metallic behavior. It is characterized by a finite Drude peak ($\sigma(\omega) \propto D\delta(\omega)$) and a corresponding $\mathcal{Q}(t) \propto iDt$ leading to a pronounced peak at $\omega = 0$ in dynamical conductivity. As t_p/t decreases, the pla-

quette orbital becomes more isolated, causing a reduction in the Drude weight. This transition culminates in the formation of a Lieb lattice with a completely flat band at $t_p = 0$ as observed in the dynamical conductivity $\text{Re}[\sigma(\omega)]$ (Fig.3), where a shift of spectral weight towards higher frequencies accompanies the diminishing Drude weight. However, this redistribution of spectral weight only marginally affects the f -sum rule. In essence, the geometric frustration decreases the band curvature $1/m_\epsilon$ and at the same time increases the geometric contribution $1/m_g$. The geometric contribution to the mass implies that there is an additional spectral weight that can flow back to zero frequency upon the inclusion of a local perturbation, for example, a local interaction, U . In sum, the flat band in the Lieb lattice is more susceptible to spectral weight transfer than a conventional flat band. A trivial atomic insulator will not feature this spectral weight transfer with interactions. The enhanced susceptibility in principle can extend to the flat band in moire materials which are also born out of geometric frustration with thousands of atoms.

V. DISCUSSION

The time-dependent Quantum Geometric Tensor offers a consistent, basis-independent framework for defining geometric properties that arise within linear response of gapped quantum systems. The real and imaginary parts of its instantaneous ($t = 0$) value determine the quantum metric and the Chern number, respectively. Through

various time derivatives, the tQGT enables a consistent definition of optical mass, orbital moment, and dielectric constants of insulators, among other quantities left to explore.

In the time domain, the tQGT exhibits bounded oscillations that correspond to zero point motion of bound electrons, which is important for properly characterizing insulators. Such oscillations are often overlooked in low-energy tight-binding models that are formulated based on *ab-initio* band structures. Nonetheless, these oscillations may become significant whenever there is a discrepancy between low-energy and local basis. This scenario is common not only in topological insulators but also in geometrically frustrated lattices and possibly moire superlattices [71–73], where the spectral weight flows to higher frequencies and shows a tendency to revert upon incorporating interactions [18, 63, 74, 75].

VI. ACKNOWLEDGEMENT

Work on quantum geometric properties of quantum materials is supported as part of Programmable Quantum Materials, an Energy Frontier Research Center funded by the U.S. Department of Energy (DOE), Office of Science, Basic Energy Sciences (BES), under award DE-SC0019443. We acknowledge discussions with Liang Fu and Yugo Onishi and thank them for discussing several aspects of their work; as well as Tobias Holder and Ilya Komissarov. The Flatiron Institute is a division of the Simons Foundation.

-
- [1] D. J. Thouless, M. Kohmoto, M. P. Nightingale, and M. den Nijs, *Phys. Rev. Lett.* **49**, 405 (1982).
 - [2] D. Vanderbilt, *Berry phases in electronic structure theory: electric polarization, orbital magnetization and topological insulators* (Cambridge University Press, 2018).
 - [3] M. Z. Hasan and C. L. Kane, *Rev. Mod. Phys.* **82**, 3045 (2010).
 - [4] X.-L. Qi and S.-C. Zhang, *Rev. Mod. Phys.* **83**, 1057 (2011).
 - [5] R. Resta, *The European Physical Journal B* **79**, 121 (2011).
 - [6] B. Bradlyn, L. Elcoro, J. Cano, M. G. Vergniory, Z. Wang, C. Felser, M. I. Aroyo, and B. A. Bernevig, *Nature* **547**:7663 **547**, 298 (2017).
 - [7] M. Vergniory, L. Elcoro, C. Felser, N. Regnault, B. A. Bernevig, and Z. Wang, *Nature* **566**, 480 (2019).
 - [8] N. Nagaosa, J. Sinova, S. Onoda, A. H. MacDonald, and N. P. Ong, *Rev. Mod. Phys.* **82**, 1539 (2010).
 - [9] D. Xiao, M.-C. Chang, and Q. Niu, *Reviews of Modern Physics* **82**, 1959 (2010).
 - [10] M. F. Lapa and T. L. Hughes, *Phys. Rev. B* **99**, 121111 (2019).
 - [11] Y. Gao and D. Xiao, *Phys. Rev. Lett.* **122**, 227402 (2019).
 - [12] V. Kozii, A. Avdoshkin, S. Zhong, and J. E. Moore, *Phys. Rev. Lett.* **126**, 156602 (2021).
 - [13] R. D. King-Smith and D. Vanderbilt, *Phys. Rev. B* **47**, 1651 (1993).
 - [14] T. Thonhauser, D. Ceresoli, D. Vanderbilt, and R. Resta, *Phys. Rev. Lett.* **95**, 137205 (2005).
 - [15] D. Xiao, J. Shi, and Q. Niu, *Phys. Rev. Lett.* **95**, 137204 (2005).
 - [16] I. Komissarov, T. Holder, and R. Queiroz, *arXiv preprint arXiv:2306.08035* (2023).
 - [17] A. Julku, S. Peotta, T. I. Vanhala, D.-H. Kim, and P. Törmä, *Phys. Rev. Lett.* **117**, 045303 (2016).
 - [18] P. Törmä, S. Peotta, and B. A. Bernevig, *Nat. Rev. Phys.* **4**, 528 (2022).
 - [19] N. Verma, T. Hazra, and M. Randeria, *Proc. Nat. Acad. Sci.* **118** (2021).
 - [20] D. Mao and D. Chowdhury, *Proc. Natl. Acad. Sci. U.S.A.* **120**, e2217816120 (2023).
 - [21] D. Mao and D. Chowdhury, *Phys. Rev. B* **109**, 024507 (2024).
 - [22] B. Hetényi and P. Lévy, *Phys. Rev. A* **108**, 032218 (2023).
 - [23] J. Ahn, G.-Y. Guo, N. Nagaosa, and A. Vishwanath, *Nat. Phys.* **18**, 290 (2022).
 - [24] M. V. Berry, *Proceedings of the Royal Society of London. A. Mathematical and Physical Sciences* **392**, 45 (1984).

- [25] J. Provost and G. Vallee, *Communications in Mathematical Physics* **76**, 289 (1980).
- [26] M. Kolodrubetz, D. Sels, P. Mehta, and A. Polkovnikov, *Physics Reports* **697**, 1 (2017).
- [27] P. Törmä, *Phys. Rev. Lett.* **131**, 240001 (2023).
- [28] T. Neupert, C. Chamon, and C. Mudry, *Phys. Rev. B* **87**, 245103 (2013).
- [29] E. Rossi, *Current Opinion in Solid State and Materials Science* **25**, 100952 (2021).
- [30] N. Verma, D. Guerci, and R. Queiroz, *arXiv preprint arXiv:2307.01253* (2023).
- [31] J. Yu, C. J. Ciccarino, R. Bianco, I. Errea, P. Narang, and B. A. Bernevig, *arXiv*, 2305.02340 (2023).
- [32] M. Iskin, *Phys. Rev. B* **107**, 224505 (2023).
- [33] J. Mitscherling and T. Holder, *Phys. Rev. B* **105**, 085154 (2022).
- [34] I. Souza, T. Wilkens, and R. M. Martin, *Phys. Rev. B* **62**, 1666 (2000).
- [35] M. Tovmasyan, S. Peotta, P. Törmä, and S. D. Huber, *Phys. Rev. B* **94**, 245149 (2016).
- [36] P. T. Mahon, J. G. Katttan, and J. E. Sipe, *Phys. Rev. B* **107**, 115110 (2023).
- [37] N. Marzari and D. Vanderbilt, *Phys. Rev. B* **56**, 12847 (1997).
- [38] N. Marzari, A. A. Mostofi, J. R. Yates, I. Souza, and D. Vanderbilt, *Rev. Mod. Phys.* **84**, 1419 (2012).
- [39] H. J. Carmichael, *Two-Level Atoms and Spontaneous Emission* (Springer, 1999) pp. 29–74.
- [40] R. Resta, *Phys. Rev. Lett.* **96**, 137601 (2006).
- [41] Y. Onishi and L. Fu, *arXiv preprint arXiv:2306.00078* (2023).
- [42] Y. Onishi and L. Fu, *arXiv preprint arXiv:2401.13847* (2024).
- [43] Y. Onishi and L. Fu, *arXiv preprint arXiv:2401.04180* (2024).
- [44] B. Ghosh, Y. Onishi, S.-Y. Xu, H. Lin, L. Fu, and A. Bansil, *arXiv preprint arXiv:2401.09689* (2024).
- [45] D. Pines and P. Nozières, *The Theory of Quantum Liquids*, Advanced Book Classics, Vol. 1 (Addison-Wesley, Redwood City, CA, 1989).
- [46] I. Souza and D. Vanderbilt, *Phys. Rev. B* **77**, 054438 (2008).
- [47] R. Resta, *Phys. Rev. Res.* **2**, 023139 (2020).
- [48] N. Ashcroft, N. Mermin, and R. Smoluchowski, *Physics Today* **30**, 61 (1977).
- [49] T. Hazra, N. Verma, and M. Randeria, *Phys. Rev. X* **9**, 031049 (2019).
- [50] G. Bellomia and R. Resta, *Phys. Rev. B* **102**, 205123 (2020).
- [51] M. Iskin, *Phys. Rev. A* **99**, 053603 (2019).
- [52] L. D. Landau, J. S. Bell, M. Kearsley, L. Pitaevskii, E. Lifshitz, and J. Sykes, *Electrodynamics of continuous media*, Vol. 8 (elsevier, 2013) p. 460.
- [53] D. Monaco, G. Panati, A. Pisante, and S. Teufel, *Communications in Mathematical Physics* **359**, 61 (2018).
- [54] A. A. Soluyanov and D. Vanderbilt, *Phys. Rev. B* **83**, 035108 (2011).
- [55] A. A. Soluyanov and D. Vanderbilt, *Phys. Rev. B* **85**, 115415 (2012).
- [56] R. Roy, *Phys. Rev. B* **90**, 165139 (2014).
- [57] P. J. Ledwith, A. Vishwanath, and D. E. Parker, *Phys. Rev. B* **108**, 205144 (2023).
- [58] P. B. Allen, *Phys. Rev. B* **92**, 054305 (2015).
- [59] W. Kohn, *Phys. Rev.* **133**, A171 (1964).
- [60] D. J. Scalapino, S. R. White, and S. Zhang, *Phys. Rev. B* **47**, 7995 (1993).
- [61] K. Seki and S. Yunoki, *Phys. Rev. B* **96**, 085124 (2017).
- [62] A. Kruchkov and S. Ryu, *arXiv preprint arXiv:2312.17318* (2023).
- [63] J. Herzog-Arbeitman, V. Peri, F. Schindler, S. D. Huber, and B. A. Bernevig, *Phys. Rev. Lett.* **128**, 087002 (2022).
- [64] J. S. Hofmann, E. Berg, and D. Chowdhury, *Phys. Rev. B* **102**, 201112 (2020).
- [65] V. Peri, Z.-D. Song, B. A. Bernevig, and S. D. Huber, *Phys. Rev. Lett.* **126**, 027002 (2021).
- [66] P. Oppeneer, *J. Magn. Magn. Mater.* **188**, 275 (1998).
- [67] M. Traini, *Eur. J. Phys.* **17**, 30 (1996).
- [68] Z. Sun, D. N. Basov, and M. M. Fogler, *Proc. Natl. Acad. Sci. U. S. A.* **115**, 3285 (2018).
- [69] Y. Cao, V. Fatemi, S. Fang, K. Watanabe, T. Taniguchi, E. Kaxiras, and P. Jarillo-Herrero, *Nature* **556**, 43 (2018).
- [70] L. Classen, *Physics* **13**, 23 (2020).
- [71] A. Julku, T. J. Peltonen, L. Liang, T. T. Heikkilä, and P. Törmä, *Phys. Rev. B* **101**, 060505 (2020).
- [72] X. Hu, T. Hyart, D. I. Pikulin, and E. Rossi, *Phys. Rev. Lett.* **123**, 237002 (2019).
- [73] J. Mendez-Valderrama, D. Mao, and D. Chowdhury, *arXiv preprint arXiv:2312.03819* (2023).
- [74] F. Xie, Z. Song, B. Lian, and B. A. Bernevig, *Phys. Rev. Lett.* **124**, 167002 (2020).
- [75] X. Hu, T. Hyart, D. I. Pikulin, and E. Rossi, *Phys. Rev. B* **105**, L140506 (2022).
- [76] B. Mera and J. Mitscherling, *Phys. Rev. B* **106**, 165133 (2022).
- [77] E. I. Blount, *Phys. Rev.* **126**, 1636 (1962).
- [78] J. E. Sipe and A. I. Shkrebtii, *Phys. Rev. B* **61**, 5337 (2000).
- [79] F. D. M. Haldane, *Phys. Rev. Lett.* **61**, 2015 (1988).

Supplementary material for “Instantaneous Response and Quantum Geometry of Insulators”

Nishchal Verma and Raquel Queiroz

Department of Physics, Columbia University, New York, NY 10027, USA

Center for Computational Quantum Physics, Flatiron Institute, New York, New York 10010, USA

Appendix A: Kubo Formula for Conductivity in Gapped Quantum Systems

We consider a generic many-body Hamiltonian \mathcal{H} in the presence of a uniform vector potential \mathbf{A} with $\mathbf{q} = 0$ and $\omega \neq 0$. Upon expanding the Hamiltonian around $\mathbf{A} = 0$, we find the paramagnetic and diamagnetic current operators:

$$j_\mu = -\frac{\delta\mathcal{H}}{\delta A_\mu} = j_{p,\mu} + A_\nu j_{d,\mu\nu} \quad (\text{A1})$$

and use linear response theory to arrive at the Kubo formula for conductivity in the exact many-body basis

$$\sigma_{\mu\nu}(\omega) = \frac{1}{i\omega} (\langle j_{d,\mu\nu} \rangle - \chi_{j_{p,\mu}, j_{p,\nu}}(\omega)) \quad (\text{A2})$$

where $\langle j_{d,\mu\nu} \rangle$ is the diamagnetic response and $\chi_{j_{p,\mu}, j_{p,\nu}}(\omega)$ is the current-current correlator. We then use the idea that the charge stiffness of the system is defined as

$$D_{\mu\nu} = \langle j_{d,\mu\nu} \rangle - \text{Re}[\chi_{j_{p,\mu}, j_{p,\nu}}(\omega = 0)] \quad (\text{A3})$$

to arrive at

$$\sigma_{\mu\nu}(\omega) = \frac{1}{i\omega} \left(D_{\mu\nu} + \text{Re}[\chi_{j_p^\mu, j_p^\nu}(\omega = 0)] - \chi_{j_p^\mu, j_p^\nu}(\omega) \right) = \frac{iD_{\mu\nu}}{\omega} - i\frac{e^2}{\hbar} \sum_{m \neq n} f_{nm} \omega_{nm} \hat{r}_\mu^{nm} \hat{r}_\nu^{mn} \frac{1}{\omega - \omega_{mn}} \quad (\text{A4})$$

where we have used an equivalent representation of the current operator in terms of position operators

$$j_\mu = \frac{e}{i\hbar} [\mathcal{H}, \hat{r}_\mu], \quad j_\mu^{mn} = \omega_{mn} \hat{r}_\mu^{nm}, \quad m \neq n \quad (\text{A5})$$

where $j_\mu^{mn} = \langle u_m | \hat{j} | u_n \rangle$ are the matrix elements of the current operator in the many-body basis.

We next note that $D_{\mu\nu}$ vanishes for gapped quantum systems that have number conservation symmetry [60]. This allows us to write the conductivity as

$$\sigma_{\mu\nu}(\omega) = -i\frac{e^2}{\hbar} \sum_{m \neq n} f_{nm} \omega_{nm} \hat{r}_\mu^{nm} \hat{r}_\nu^{mn} \frac{1}{\omega - \omega_{mn}} \quad (\text{A6})$$

where f_n is the occupation of energy ω_n and

$$f_{nm} \equiv f_n - f_m, \quad \omega_{mn} \equiv \omega_m - \omega_n, \quad \hat{r}_\mu^{nm} \equiv \langle u_n | \hat{r}_\mu | u_m \rangle. \quad (\text{A7})$$

We emphasize that the Eq. (A6) is formally true even with interactions and disorder. The advantage of using position matrix elements instead of current will become clear when we split the position vectors into symmetric and anti-symmetric parts

$$\hat{r}_\mu^{nm} \hat{r}_\nu^{mn} = g_{\mu\nu}^{nm} + \frac{i}{2} \Omega_{\mu\nu}^{nm} \quad (\text{A8})$$

with

$$g_{\mu\nu}^{nm} = \frac{1}{2} (\hat{r}_\mu^{nm} \hat{r}_\nu^{mn} + \hat{r}_\nu^{nm} \hat{r}_\mu^{mn}), \quad i\Omega_{\mu\nu}^{nm} = \hat{r}_\mu^{nm} \hat{r}_\nu^{mn} - \hat{r}_\nu^{nm} \hat{r}_\mu^{mn}. \quad (\text{A9})$$

Note that g is symmetric under $\mu \leftrightarrow \nu$ as well as $n \leftrightarrow m$ while Ω is anti-symmetric for both. The notation is chosen this way since the matrix elements add up to the quantum metric and Berry curvature for a given state:

$$g_{\mu\nu}^n = \sum_{m \neq n} g_{\mu\nu}^{nm}, \quad \Omega_{\mu\nu}^n = \sum_{m \neq n} \Omega_{\mu\nu}^{nm}. \quad (\text{A10})$$

This decomposition allows a succinct representation of conductivity that explicitly shows the quantum geometric content that is usually hidden in the position operators

$$\sigma_{\mu\nu}(\omega) = -i \frac{e^2}{\hbar} \sum_{m \neq n} f_{nm} \omega_{nm} (g_{\mu\nu}^{nm} + i\Omega_{\mu\nu}^{nm}/2) \frac{1}{\omega - \omega_{mn}}. \quad (\text{A11})$$

We note that although quantum geometry makes an appearance in the Kubo formula, extracting a precise observable that tracks it is quite complicated.

1. Dissipative and Reactive Components in Insulators

We use the standard Sokhotski–Plemelj theorem to write

$$\frac{1}{\omega - \omega_{mn}} = \mathcal{P} \left[\frac{1}{\omega - \omega_{mn}} \right] - i\pi\delta(\omega - \omega_{mn}), \quad (\text{A12})$$

where \mathcal{P} denotes the Cauchy principle value. As a reminder, note that this decomposition is done in the exact many-body basis which already includes effects of interactions and disorder. We next rewrite conductivity in Eq. (A11) as

$$\sigma_{\mu\nu}(\omega) = -i \frac{e^2}{\hbar} \sum_{m \neq n} f_{nm} \omega_{nm} (g_{\mu\nu}^{nm} + i\Omega_{\mu\nu}^{nm}/2) \left(\mathcal{P} \left[\frac{1}{\omega - \omega_{mn}} \right] - i\pi\delta(\omega - \omega_{mn}) \right) \quad (\text{A13})$$

whose real and imaginary parts are

$$\text{Re}[\sigma_{\mu\nu}(\omega)] = \frac{e^2}{2\hbar} \sum_{m \neq n} f_{nm} \omega_{mn} \left(2\pi g_{\mu\nu}^{nm} \delta(\omega - \omega_{mn}) - \Omega_{\mu\nu}^{nm} \mathcal{P} \left[\frac{1}{\omega - \omega_{mn}} \right] \right) \quad (\text{A14a})$$

$$\text{Im}[\sigma_{\mu\nu}(\omega)] = \frac{e^2}{2\hbar} \sum_{m \neq n} f_{nm} \omega_{mn} \left(\pi \Omega_{\mu\nu}^{nm} \delta(\omega - \omega_{mn}) - 2g_{\mu\nu}^{nm} \mathcal{P} \left[\frac{1}{\omega - \omega_{mn}} \right] \right). \quad (\text{A14b})$$

The real and imaginary parts of conductivity have both dissipative (with $\delta(x)$ functions) and reactive (with principle value) components. While our main focus is on the dissipative part and their corresponding sum rules, it is beneficial to note that the reactive part yields the well known TKNN formula. In the dc limit, $\omega = 0$, we get

$$\text{Re}[\sigma_{\mu\nu}(0)] = \frac{e^2}{\hbar} \sum_{m \neq n} f_{nm} \Omega_{\mu\nu}^{mn}/2 = \frac{e^2}{2\hbar} \epsilon_{\mu\nu} \mathcal{C}, \quad \text{Im}[\sigma_{\mu\nu}(0)] = \frac{e^2}{2\hbar} \sum_{m \neq n} f_{nm} g_{\mu\nu}^{mn} = 0 \quad (\text{A15})$$

where \mathcal{C} is the Chern number and $\epsilon_{\mu\nu}$ is the Levi-Civita tensor. This is the TKNN formula for Hall conductivity $\sigma_H = \sigma_{xy} - \sigma_{yx} = (e^2/\hbar)\mathcal{C}$ [1]. It is the first instance where quantum geometry directly leads to an observable in conductivity without making any assumptions about band energies.

Appendix B: Conductivity in time domain

Intuitively, conductivity arises from the motion of charges. Since charges are frozen in insulators, the naive expectation is that insulators will have trivial dynamics. It is however interesting to analyze the motion from a perspective of quantum geometry. The conductivity in the time domain is merely a Fourier transform of Eq. (A11)

$$\sigma_{\mu\nu}(t) = \int_{-\infty}^{\infty} d\omega e^{i\omega t} \sigma_{\mu\nu}(\omega) = \frac{2\pi e^2}{\hbar} \sum_{m \neq n} f_{nm} \omega_{nm} (g_{\mu\nu}^{nm} + i\Omega_{\mu\nu}^{nm}/2) \left[\int_{-\infty}^{\infty} \frac{d\omega}{2\pi i} \frac{e^{i\omega t}}{\omega - \omega_{mn}} \right] \quad (\text{B1})$$

$$= \frac{2\pi e^2}{\hbar} \Theta(t) \sum_{m \neq n} f_{nm} \omega_{nm} (g_{\mu\nu}^{nm} + i\Omega_{\mu\nu}^{nm}/2) e^{i\omega_{mn} t} \quad (\text{B2})$$

which we can further simplify as

$$\sigma_{\mu\nu}(t) = \frac{2\pi e^2}{\hbar} \Theta(t) \sum_{m \neq n} f_{nm} \omega_{nm} [g_{\mu\nu}^{nm} \cos(\omega_{mn}t) - \Omega_{\mu\nu}^{nm} \sin(\omega_{mn}t)/2] \quad (\text{B3})$$

so that it is explicit that $\sigma_{\mu\nu}(t)$ is a real number. The equation has a consistent structure with symmetric part g_{mn} appearing with symmetric $\cos(\omega_{mn}t)$ and vice versa. We can make an attempt to extract the band resolved quantum geometry

$$\sigma_{\mu\nu}(t) = \frac{2\pi e^2}{\hbar} \Theta(t) \sum_n f_n \left(\sum_{m \neq n} \omega_{nm} [g_{\mu\nu}^{nm} \cos(\omega_{mn}t) - \Omega_{\mu\nu}^{nm} \sin(\omega_{mn}t)/2] \right) \quad (\text{B4})$$

but the term inside the bracket is off by a factor of ω_{mn} , in comparison to the definition of quantum metric and Berry curvature in Eq. (A10). This motivates us to endow time-dependence to quantum geometry that may potentially induce factors of ω_{mn} . We will explore this in the next section.

Appendix C: Time Dependent Quantum Geometric Tensor

We introduce the time-dependent quantum geometric tensor as a quantity of interest in its own right. The off-diagonal dipole operator, $\mathcal{D}_\mu(t) = \hat{Q} \hat{r}_\mu(t) \hat{P}$ causes transitions between the occupied states (described by \hat{P}) and unoccupied states (described by \hat{Q}), and $\mathcal{D}_\mu^\dagger(t)$ does the inverse. The time-dependent Quantum Geometric Tensor (tQGT) is defined as the correlation function

$$\mathcal{Q}_{\mu\nu}(t-t') = \langle \mathcal{D}_\mu^\dagger(t) \mathcal{D}_\nu(t') \rangle = \langle \hat{P} \hat{r}_\mu(t) \hat{Q} \hat{r}_\nu(0) \rangle \quad (\text{C1})$$

where we can use the fact that thermal expectation values are taken with $\langle \hat{O} \rangle = \text{Tr}[\hat{\rho} \hat{O}]$ where $\hat{\rho}$ is the density matrix that is diagonal in the eigenstate representation. We get

$$\mathcal{Q}_{\mu\nu}(t-t') = \sum_{m \neq n} f_n (1-f_m) e^{i\omega_{mn}t} \hat{r}_\mu^{nm} \hat{r}_\nu^{mn} \quad (\text{C2})$$

where $\{f_n\}$ are the thermal occupation factors. As noted in the main text, tQGT describes correlation between dipole moments mediated entirely via virtual states. The correlation function is inherently quantum in nature and will vanish identically for classical systems at zero temperature. We next use the decomposition of position operators from Eq. (A8) to write it as

$$\mathcal{Q}_{\mu\nu}(t) = \sum_{m \neq n} f_n (1-f_m) e^{i\omega_{mn}t} (g_{\mu\nu}^{mn} + i\Omega_{\mu\nu}^{mn}/2). \quad (\text{C3})$$

The tensor has several interesting properties. At $t=0$, it is equal to the quantum geometric tensor whose real and imaginary parts are the quantum metric and Berry curvature

$$\mathcal{Q}_{\mu\nu}(t=0) = \left(\sum_{m \neq n} f_n (1-f_m) g_{\mu\nu}^{mn} \right) + \frac{i}{2} \left(\sum_{m \neq n} f_n (1-f_m) \Omega_{\mu\nu}^{mn} \right). \quad (\text{C4})$$

Note that the quantum metric of the filled states is not the sum of individual quantum metrics for each state. It is not additive [76], unlike the Chern number.

At finite t , the presence of complimentary projector \hat{Q} in Eq. (C2) destroys the Hermiticity with $\mathcal{Q}_{\mu\nu}(t)^\dagger = \mathcal{Q}_{\nu\mu}(-t)$. However, we can always split it into Hermitian and anti-Hermitian components

$$\mathcal{Q}_{\mu\nu}(t) = \frac{1}{2} (\mathcal{Q}_{\mu\nu}(t) + \mathcal{Q}_{\nu\mu}(-t)) + \frac{1}{2} (\mathcal{Q}_{\mu\nu}(t) - \mathcal{Q}_{\nu\mu}(-t)) \equiv \mathcal{Q}_{\mu\nu}^s(t) - \frac{i}{2} \mathcal{Q}_{\mu\nu}^{\text{as}}(t) \quad (\text{C5})$$

which introduces Hermitian tensors

$$\mathcal{Q}_{\mu\nu}^s(t) = \sum_{m \neq n} f_n (1-f_m) [\cos(\omega_{mn}t) g_{\mu\nu}^{mn} - \sin(\omega_{mn}t) \Omega_{\mu\nu}^{mn}/2] \quad (\text{C6})$$

$$\mathcal{Q}_{\mu\nu}^{\text{as}}(t) = \sum_{m \neq n} f_n (1-f_m) [2 \sin(\omega_{mn}t) g_{\mu\nu}^{mn} + \cos(\omega_{mn}t) \Omega_{\mu\nu}^{mn}]. \quad (\text{C7})$$

These quantities oscillate between quantum geometry and Berry curvature. More importantly, they reformulate the zero point dynamics of charge to the presence of quantum metric and Berry curvature.

Returning to our goal of making connections with conductivity, we note that $\mathcal{Q}_{\mu\nu}^{\text{as}}$ can be rewritten as

$$\mathcal{Q}_{\mu\nu}^{\text{as}}(t) = 2 \sum_{m \neq n} f_{nm} [\sin(\omega_{mn}t)g_{\mu\nu}^{mn} + \cos(\omega_{mn}t)\Omega_{\mu\nu}^{mn}/2] \quad (\text{C8})$$

so that upon taking a time derivative

$$\partial_t \mathcal{Q}_{\mu\nu}^{\text{as}}(t) = 2 \sum_{m \neq n} f_{nm}\omega_{mn} [\cos(\omega_{mn}t)g_{\mu\nu}^{mn} - \sin(\omega_{mn}t)\Omega_{\mu\nu}^{mn}/2] \quad (\text{C9})$$

we get an expression that is identical to conductivity in the time domain in Eq. (B3). This leads us to the exact relation

$$\sigma_{\mu\nu}(t) = \frac{\pi e^2}{\hbar} \Theta(t) \partial_t \mathcal{Q}_{\mu\nu}^{\text{as}}(t). \quad (\text{C10})$$

Appendix D: Time Dependent Quantum Geometry in Crystalline solids

In this section, we evaluate tQGT for crystalline solids that have eigenstates that are resolved into band n and crystal momentum \mathbf{k} defined in the Brillouin Zone (BZ). We begin with the projectors that are given by

$$\hat{P} = \int_{\text{BZ}} d\mathbf{k} \sum_n f_{n,\mathbf{k}} |u_{n,\mathbf{k}}\rangle \langle u_{n,\mathbf{k}}|, \quad \hat{Q} = \int_{\text{BZ}} d\mathbf{k}' \sum_m (1 - f_{m,\mathbf{k}'}) |u_{m,\mathbf{k}'}\rangle \langle u_{m,\mathbf{k}'}| \quad (\text{D1})$$

where $f_{n,\mathbf{k}}$ is the Fermi occupation factor and $\{|u_{m,\mathbf{k}'}\rangle\}$ are the cell-periodic parts of the Bloch wavefunctions. Putting it all together in Eq. (C2), we get

$$\mathcal{Q}_{\mu\nu}(t) = \int_{\text{BZ}} d\mathbf{k} d\mathbf{k}' \sum_{m,n} f_{n,\mathbf{k}} (1 - f_{m,\mathbf{k}'}) \langle u_{n,\mathbf{k}} | \hat{r}_\mu | u_{m,\mathbf{k}'} \rangle \langle u_{m,\mathbf{k}'} | \hat{r}_\nu | u_{n,\mathbf{k}} \rangle e^{i(\omega_{m,\mathbf{k}'} - \omega_{n,\mathbf{k}})t} \quad (\text{D2})$$

where the matrix elements of the position operator have a definite structure [77, 78]

$$\langle u_{n,\mathbf{k}} | \hat{r}_\mu | u_{m,\mathbf{k}'} \rangle = \delta_{mn} (-\hbar \delta(\mathbf{k} - \mathbf{k}') \langle u_{n,\mathbf{k}} | i\partial_\mu u_{m,\mathbf{k}'} \rangle + i\hbar \partial_\mu \delta(\mathbf{k} - \mathbf{k}')) + (1 - \delta_{mn}) \delta(\mathbf{k} - \mathbf{k}') \langle u_{n,\mathbf{k}} | i\partial_\mu u_{m,\mathbf{k}'} \rangle. \quad (\text{D3})$$

that leads to three different terms in tQGT

$$\mathcal{Q}_{\mu\nu}(t) = \mathcal{Q}_{\mu\nu}^{\text{inter}}(t) + \mathcal{Q}_{\mu\nu}^{\text{intra}}(t) + \tilde{\mathcal{Q}}_{\mu\nu}^{\text{intra}} \quad (\text{D4})$$

with the superscripts ‘‘inter’’ referring to inter-band, ‘‘intra’’ with a tilde referring to gauge dependent intra-band, and ‘‘intra’’ referring to gauge independent intra-band terms.

1. Inter-Band Contribution

Inter-band position matrix elements have a delta function in momentum that makes $\langle u_{n,\mathbf{k}} | i\partial_\mu u_{m,\mathbf{k}} \rangle$ momentum diagonal and we get

$$\mathcal{Q}_{\mu\nu}^{\text{inter}}(t) = \int_{\text{BZ}} d\mathbf{k} f_{n,\mathbf{k}} (1 - f_{m,\mathbf{k}}) \langle u_{n,\mathbf{k}} | i\partial_\mu u_{m,\mathbf{k}} \rangle \langle u_{m,\mathbf{k}} | i\partial_\nu u_{n,\mathbf{k}} \rangle e^{i\omega_{mn,\mathbf{k}}t} \quad (\text{D5})$$

which is identical to Eq. (C3), with the additional label and integral over \mathbf{k} .

2. Intra-Band Contribution

We identify the diagonal matrix element $\langle u_{m,\mathbf{k}} | i\partial_\mu u_{m,\mathbf{k}} \rangle \equiv \mathcal{A}_m^\mu(\mathbf{k})$ as the Berry connection. The gauge-dependent part of the tQGT can now be easily inferred

$$\tilde{\mathcal{Q}}_{\mu\nu}^{\text{intra}}(t) = -\hbar \int_{\text{BZ}} d\mathbf{k} \sum_m f_{m,\mathbf{k}}(1 - f_{m,\mathbf{k}}) \mathcal{A}_m^\mu(\mathbf{k}) \mathcal{A}_m^\nu(\mathbf{k}). \quad (\text{D6})$$

Note that the contribution is time-independent and is symmetric in μ, ν . It drops out of the anti-symmetric part of tQGT and does not appear in any observable.

The other intra-band component of tQGT maps to a Fermi-surface contribution. To see that, we use the alternate expression of the position operator in terms of the current operator

$$\langle u_{m,\mathbf{k}'} | \hat{r}_\nu | u_{m,\mathbf{k}} \rangle = \frac{\langle u_{m,\mathbf{k}'} | \hat{J}_\nu | u_{m,\mathbf{k}} \rangle}{\omega_{m,\mathbf{k}} - \omega_{m,\mathbf{k}'}} , \quad \mathbf{k} \neq \mathbf{k}'. \quad (\text{D7})$$

in one of the position operators in Eq. (C2) to get

$$\mathcal{Q}_{\mu\nu}^{\text{intra}}(t) = i\hbar \int_{\text{BZ}} d\mathbf{k} d\mathbf{k}' \sum_m f_{m,\mathbf{k}}(1 - f_{m,\mathbf{k}'}) (\partial_\mu \delta(\mathbf{k} - \mathbf{k}')) \frac{\langle u_{m,\mathbf{k}'} | \hat{J}_\nu | u_{m,\mathbf{k}} \rangle}{\omega_{m,\mathbf{k}} - \omega_{m,\mathbf{k}'}} e^{i\omega_{m,\mathbf{k}',\mathbf{k}}t}. \quad (\text{D8})$$

where $\omega_{m,\mathbf{k}',\mathbf{k}} \equiv \omega_{m,\mathbf{k}'} - \omega_{m,\mathbf{k}}$. We find it convenient to rewrite the expression as

$$\mathcal{Q}_{\mu\nu}^{\text{intra}}(t) = i \int_{\text{BZ}} d\mathbf{k} d\mathbf{k}' \sum_m \frac{f_{m,\mathbf{k}} - f_{m,\mathbf{k}'}}{\omega_{m,\mathbf{k}} - \omega_{m,\mathbf{k}'}} \partial_\mu \delta(\mathbf{k} - \mathbf{k}') \left(\langle u_{m,\mathbf{k}'} | \hat{J}_\nu | u_{m,\mathbf{k}} \rangle e^{i\omega_{m,\mathbf{k}',\mathbf{k}}t} - \langle u_{m,\mathbf{k}} | \hat{J}_\nu | u_{m,\mathbf{k}'} \rangle e^{-i\omega_{m,\mathbf{k}',\mathbf{k}}t} \right). \quad (\text{D9})$$

The next step is to use integration by parts in the delta function

$$\int d\mathbf{x} \partial_\mu \delta(\mathbf{x} - \mathbf{x}_0) f(\mathbf{x}) = - \int d\mathbf{x} \delta(\mathbf{x} - \mathbf{x}_0) \partial_\mu f(\mathbf{x}) = -\partial_\mu f(\mathbf{x}_0). \quad (\text{D10})$$

The trick here is to note that the term inside the big bracket in Eq. (D9) vanishes when $\mathbf{k} = \mathbf{k}'$. Hence, the only term that survives after the integration by parts is one that has derivatives of the phases $e^{-i\omega_{m,\mathbf{k}',\mathbf{k}}t}$. With this insight, we get

$$\mathcal{Q}_{\mu\nu}^{\text{intra}}(t) = i \sum_m \left(\lim_{\mathbf{k} \rightarrow \mathbf{k}'} \frac{f_{m,\mathbf{k}} - f_{m,\mathbf{k}'}}{\omega_{m,\mathbf{k}} - \omega_{m,\mathbf{k}'}} \right) \langle u_{m,\mathbf{k}} | \hat{J}_\nu | u_{m,\mathbf{k}} \rangle \left(\partial_\mu e^{i(\omega_{m,\mathbf{k}'} - \omega_{m,\mathbf{k}})t} - \partial_\mu e^{-i(\omega_{m,\mathbf{k}'} - \omega_{m,\mathbf{k}})t} \right)_{\mathbf{k}=\mathbf{k}'} \quad (\text{D11a})$$

$$= t \sum_m \left(-\frac{\partial f}{\partial \omega} \right)_{\omega=\omega_{m,\mathbf{k}}} \partial_\nu \omega_{m,\mathbf{k}} \partial_\mu \omega_{m,\mathbf{k}} \equiv D_{\mu\nu} t \quad (\text{D11b})$$

where we have defined Drude weight $D_{\mu\nu}$ as

$$D_{\mu\nu} = \sum_m \left(-\frac{\partial f}{\partial \omega} \right)_{\omega=\omega_{m,\mathbf{k}}} \partial_\nu \omega_{m,\mathbf{k}} \partial_\mu \omega_{m,\mathbf{k}} \propto N(0) \langle v_F^2 \rangle_{\text{FS}} \quad (\text{D12})$$

where $N(0)$ is the density of states at the Fermi level and v_F is the Fermi velocity averaged $\langle \cdot \rangle$ over the Fermi surface.

3. Relation to Conductivity and Drude peak

With all three terms in place, the tQGT is

$$\mathcal{Q}_{\mu\nu}(t) = \int_{\text{BZ}} \sum_{m \neq n} f_{n,\mathbf{k}}(1 - f_{m,\mathbf{k}}) \hat{r}_\mu^{nm} \hat{r}_\nu^{mn} e^{i\omega_{mn,\mathbf{k}}t} + D_{\mu\nu} t - \hbar \int_{\text{BZ}} \sum_m f_{m,\mathbf{k}}(1 - f_{m,\mathbf{k}}) \mathcal{A}_m^\mu(\mathbf{k}) \mathcal{A}_m^\nu(\mathbf{k}) \quad (\text{D13})$$

As we showed earlier, conductivity is related to the anti-symmetric part

$$\mathcal{Q}_{\mu\nu}^{\text{as}}(t) = i(\mathcal{Q}_{\mu\nu}(t) - \mathcal{Q}_{\nu\mu}(-t)) = iD_{\mu\nu} t + \int_{\text{BZ}} \sum_{m \neq n} f_{n,\mathbf{k}}(1 - f_{m,\mathbf{k}}) [\sin(\omega_{mn,\mathbf{k}}t) g_{\mu\nu}^{mn}(\mathbf{k}) + \cos(\omega_{mn,\mathbf{k}}t) \Omega_{\mu\nu}^{mn}(\mathbf{k})/2] \quad (\text{D14})$$

and in particular, conductivity is given by

$$\begin{aligned}\sigma_{\mu\nu}(t) &= \frac{2\pi e^2}{\hbar} \Theta(t) \partial_t \mathcal{Q}_{\mu\nu}^{\text{as}} \tag{D15} \\ &= \frac{2\pi e^2}{\hbar} \Theta(t) \left(2iD_{\mu\nu} + \int_{\text{BZ}} \sum_{m \neq n} f_{n,\mathbf{k}} (1 - f_{m,\mathbf{k}}) \omega_{mn,\mathbf{k}} [\cos(\omega_{mn,\mathbf{k}} t) g_{\mu\nu}^{mn}(\mathbf{k}) - \sin(\omega_{mn,\mathbf{k}} t) \Omega_{\mu\nu}^{mn}(\mathbf{k})/2] \right) \tag{D16}\end{aligned}$$

which is identical to the expression for gapped systems, except for the Fermi-surface term, $D_{\mu\nu}$, and the inclusion of the momentum label \mathbf{k} .

Appendix E: Conductivity in Axial Vector Notation

The discussion so far has been very general and most equations have been written down for arbitrary spatial directions μ, ν . In the upcoming sections, we will use dissipative parts of conductivity which require specific spatial directions. We begin by splitting conductivity into symmetric and anti-symmetric parts

$$\sigma_{\mu\nu}(\omega) = \frac{1}{2}(\sigma_{\mu\nu}(\omega) + \sigma_{\nu\mu}(\omega)) + \left(\frac{1}{2}(\sigma_{\mu\nu}(\omega) - \sigma_{\nu\mu}(\omega)) \right) \tag{E1}$$

and then define the axial vectors σ_L and σ_H to absorb the two

$$\sigma_{\mu\nu}(\omega) = \delta_{\mu\nu} \sigma_{L,\mu}(\omega) + \epsilon_{\mu\nu\lambda} \sigma_{H,\lambda}(\omega). \tag{E2}$$

In 3D, there are three components to σ_L (for x, y, z) and three σ_H (for xy, yz, xz), whereas in 2D, there are two components in σ_L but only one in σ_H (xy). In the case of an applied magnetic field, $\hat{\lambda}$ is along the direction of the magnetic field.

We now introduce the absorptive part of conductivity

$$\sigma^{\text{abs}} = \frac{1}{2}(\sigma_{\mu\nu} + \sigma_{\nu\mu}^*) = \frac{1}{2}(\delta_{\mu\nu} \sigma_{L,\mu}(\omega) + \epsilon_{\mu\nu\lambda} \sigma_{H,\lambda}(\omega) + \delta_{\mu\nu} \sigma_{L,\mu}^*(\omega) - \epsilon_{\mu\nu\lambda} \sigma_{H,\lambda}^*(\omega)) \tag{E3a}$$

$$= \delta_{\mu\nu} \frac{1}{2}(\sigma_{L,\mu}(\omega) + \sigma_{L,\mu}^*(\omega)) + \epsilon_{\mu\nu\lambda} \frac{1}{2}(\sigma_{H,\lambda}(\omega) - \sigma_{H,\lambda}^*(\omega)) \tag{E3b}$$

$$= \delta_{\mu\nu} \text{Re}[\sigma_{L,\mu}(\omega)] + i\epsilon_{\mu\nu\lambda} \text{Im}[\sigma_{H,\lambda}(\omega)] \tag{E3c}$$

which will eventually give rise to sum rules.

Lastly, we introduce axial vectors for position matrix elements

$$g_{\mu\nu}^{nm} = g_{\mu}^{nm} \delta_{\mu\nu}, \quad \Omega_{\mu\nu}^{nm} = 2\epsilon_{\mu\nu\lambda} \Omega_{\lambda}^{nm} \tag{E4}$$

to facilitate the discussion on sum rules of dissipative response functions in the upcoming sections.

Appendix F: tQGT and Sum Rules of Dissipative Response

We begin by considering the absorptive part of conductivity

$$\sigma^{\text{abs}} = \delta_{\mu\nu} \text{Re}[\sigma_{L,\mu}(\omega)] + i\epsilon_{\mu\nu\lambda} \text{Im}[\sigma_{H,\lambda}(\omega)] = \frac{\pi e^2}{\hbar} \sum_{m \neq n} f_{nm} \omega_{mn} (g_{\mu}^{mn} \delta_{\mu\nu} + i\epsilon_{\mu\nu\lambda} \Omega_{\lambda}^{mn}) \delta(\omega - \omega_{mn}). \tag{F1}$$

and the generalized sum rules

$$\mathcal{S}_{\mu\nu}^{\eta} = \int_0^{\infty} d\omega \frac{\sigma_{\mu\nu}^{\text{abs}}(\omega)}{\omega^{1-\eta}} = \frac{\pi e^2}{\hbar} \sum_{m \neq n} f_{nm} \omega_{mn} (g_{\mu}^{mn} \delta_{\mu\nu} + i\epsilon_{\mu\nu\lambda} \Omega_{\lambda}^{mn}) \left[\int_0^{\infty} d\omega \frac{\delta(\omega - \omega_{mn})}{\omega^{1-\eta}} \right] \tag{F2}$$

where the frequency integral is given by $\Theta(\omega_{mn})/2\omega_{mn}^{1-\eta}$. The Θ function enters because the limits of the integral only access the positive peaks. The resulting sum rule is

$$\mathcal{S}_{\mu\nu}^{\eta} = \frac{\pi e^2}{\hbar} \sum_{m \neq n} f_{nm} \omega_{mn}^{\eta} (g_{\mu}^{mn} \delta_{\mu\nu} + i\epsilon_{\mu\nu\lambda} \Omega_{\lambda}^{mn}) \Theta(\omega_{mn}). \tag{F3}$$

To link this sum rule with the quantum geometric tensor, we refine the expression by writing the occupation factor f_{nm} as $f_{nm} = f_n(1 - f_m) - f_m(1 - f_n)$. We then split the sum into two parts and swap $m \leftrightarrow n$ in the second sum. After combining the two we get

$$\frac{\pi e^2}{\hbar} \sum_{m \neq n} f_n(1 - f_m) \omega_{mn}^\eta ((g_\mu^{mn} \delta_{\mu\nu} + i \epsilon_{\mu\nu\lambda} \Omega_\lambda^{mn}) \Theta(\omega_{mn}) - (-1)^\eta (g_\mu^{mn} \delta_{\mu\nu} + i \epsilon_{\mu\nu\lambda} \Omega_\lambda^{mn}) \Theta(-\omega_{mn})) \quad (\text{F4})$$

which is best expressed in longitudinal and Hall parts separately

$$\mathcal{S}_{L,\mu}^\eta = \frac{\pi e^2}{\hbar} \sum_{m \neq n} f_n(1 - f_m) \omega_{mn}^\eta g_\mu^{mn} (\Theta(\omega_{mn}) - (-1)^\eta \Theta(-\omega_{mn})) \quad (\text{F5a})$$

$$\mathcal{S}_{H,\lambda}^\eta = \frac{\pi e^2}{\hbar} \sum_{m \neq n} f_n(1 - f_m) \omega_{mn}^\eta \Omega_\lambda^{mn} (\Theta(\omega_{mn}) + (-1)^\eta \Theta(-\omega_{mn})). \quad (\text{F5b})$$

The $\Theta(\omega_{mn})$ factors select only half of the resonances. This is crucial for sum rules whose integrand is odd in frequency, which would otherwise cancel if integrated over the full $-\infty$ to ∞ range. Taking advantage of the gapped spectrum, at $T = 0$, with $f_n = 1$ for filled states and 0 otherwise, we naturally obtain positive ω_{mn} . This action forbids us from using $m \leftrightarrow n$ tricks in the future but simplifies the sum rule to the concise expression

$$\mathcal{S}_{L,\mu}^\eta = \frac{\pi e^2}{\hbar} \sum_{m \neq n} f_n(1 - f_m) \omega_{mn}^\eta g_\mu^{mn}, \quad \mathcal{S}_{H,\lambda}^\eta = \frac{\pi e^2}{\hbar} \sum_{m \neq n} f_n(1 - f_m) \omega_{mn}^\eta \Omega_\lambda^{mn}, \quad (\text{F6})$$

which we will now relate to the geometric tensor. We first need to extend the L and H terminology to the geometric tensor. We define

$$\mathcal{Q}_{\mu\nu}(t) = \sum_{m \neq n} f_n(1 - f_m) e^{i\omega_{mn}t} (g_\mu^{mn} \delta_{\mu\nu} + \epsilon_{\mu\nu\lambda} \Omega_\lambda^{mn}) \quad (\text{F7})$$

to finally arrive at

$$\mathcal{S}_{L/H,\mu}^\eta = \frac{\pi e^2}{\hbar} \left[(-i\hat{\partial}_t)^\eta \mathcal{Q}_{L/H,\mu}(t) \right]_{t=0} \quad (\text{F8})$$

which explicitly shows that the time-dependent quantum geometric tensor is a generating function for all sum rules.

1. $\eta = 0$ SWM Sum Rule

We begin with the simplest observation that $\eta = 0$ recovers the SWM sum rule

$$\mathcal{S}_{L,\mu}^0 = \int_0^\infty d\omega \frac{\text{Re}[\sigma_{L,\mu}(\omega)]}{\omega} = \frac{\pi e^2}{\hbar} \text{Tr}[g_\mu], \quad \mathcal{S}_{H,\lambda}^0 = \int_0^\infty d\omega \frac{\text{Re}[\sigma_{H,\lambda}(\omega)]}{\omega} = \frac{\pi e^2}{\hbar} \mathcal{C}_\lambda, \quad (\text{F9})$$

where $\text{Tr}[g_\mu]$ is the quantum metric and \mathcal{C}_λ is the Chern number of the occupied bands. Remarkably, the negative moment can extract the quantum geometry of the system.

2. $\eta = 1$ f -Sum Rule

The $\eta = 1$ sum rule defines two distinct physical quantities: optical mass from longitudinal and magnetic moment from Hall.

- Longitudinal sum rule defines optical mass

$$\int_0^\infty d\omega \text{Re}[\sigma_{L,\mu}(\omega)] = \frac{\pi e^2}{\hbar} \sum_{m \neq n} f_n(1 - f_m) \omega_{mn} g_\mu^{mn} \quad (\text{F10})$$

where we can further use the fact that $\omega_{mn}g_{mn}$ is anti-symmetric in $m \leftrightarrow n$ to get

$$\int_0^\infty d\omega \operatorname{Re}[\sigma_{L,\mu}(\omega)] = \frac{\pi e^2}{\hbar} \sum_n f_n \left(\sum_{m \neq n} \omega_{mn} g_\mu^{mn} \right) \quad (\text{F11})$$

where the quantity in brackets defines an effective mass for the a band

$$[\mathcal{M}_n^{-1}]_\mu = \sum_{m \neq n} \omega_{mn} g_\mu^{mn} \quad (\text{F12})$$

going with analogy that the f -sum rule gives the plasma frequency that takes the form n/m^* with some effective mass m^* . Here we are finding that m^* is indeed related to the quantum geometry. Moreover, the mass can be resolved for each band n and momenta \mathbf{k} . Lastly, we note that in metals, the Fermi-surface modifies the effective mass with the band curvature as we saw already in sec. D 2. The additional contribution is the Drude piece

$$D_{\mu\nu} = \int_{\text{BZ}} d\mathbf{k} \sum_m \left(-\frac{\partial f}{\partial \omega} \right)_{\omega=\omega_{m,\mathbf{k}}} \partial_\nu \omega_{m,\mathbf{k}} \partial_\mu \omega_{m,\mathbf{k}} = \int_{\text{BZ}} d\mathbf{k} \sum_m f_{m,\mathbf{k}} \partial_{\mu\nu}^2 \epsilon_{m,\mathbf{k}} \quad (\text{F13})$$

which gives the full sum rule

$$\int_0^\infty d\omega \operatorname{Re}[\sigma_{L,\mu}(\omega)] = \frac{\pi e^2}{\hbar} \int_{\text{BZ}} d\mathbf{k} \sum_m f_{m,\mathbf{k}} (\partial_\mu^2 \epsilon_{m,\mathbf{k}} + [\mathcal{M}_m^{-1}(\mathbf{k})]_\mu) \quad (\text{F14})$$

which was used in ref. [49] to get upper bounds on superfluid stiffness in multi-band systems.

- Hall sum rule defines magnetic moment

$$\int_0^\infty d\omega \operatorname{Im}[\sigma_{H,\lambda}(\omega)] = \frac{\pi e^2}{\hbar} \sum_{m \neq n} f_n (1 - f_m) \omega_{mn} \Omega_\lambda^{mn} \quad (\text{F15})$$

where

$$\mu^\lambda = \sum_{\substack{n \in \text{filled} \\ m \in \text{empty}}} \omega_{mn} \Omega_\lambda^{mn} \quad (\text{F16})$$

is defined to be the net orbital magnetic moment of the filled bands (see eq. (12) in Ref. [46]).

3. $\eta = -1$ Dielectric Permittivity

The longitudinal response

$$\int_0^\infty d\omega \frac{\operatorname{Re}[\sigma_{L,\mu}(\omega)]}{\omega^2} = \frac{\pi e^2}{\hbar} \sum_{m \neq n} f_n (1 - f_m) \frac{g_\mu^{mn}}{\omega_{mn}} = \frac{\pi e^2}{\hbar} \sum_{m \neq n} f_n \left(\sum_{m \neq n} \frac{g_\mu^{mn}}{\omega_{mn}} \right) \quad (\text{F17})$$

defines the electric susceptibility of the n^{th} band as

$$\chi_\mu^{e,n} = \sum_{\substack{n \in \text{filled} \\ m \in \text{empty}}} \frac{g_\mu^{mn}}{\omega_{mn}} \quad (\text{F18})$$

related to the capacitance by the vacuum permittivity $c_\mu^{e,n} = \epsilon_0 \chi_\mu^{e,n}$. Similarly, the Hall response is obtained by the nonreciprocal part of the sum rule, only present if time-reversal symmetry is broken

$$\int_0^\infty d\omega \frac{\operatorname{Im}[\sigma_{H,\lambda}(\omega)]}{\omega^2} = \frac{\pi e^2}{\hbar} \sum_{m \neq n} f_n (1 - f_m) \frac{\Omega_\lambda^{mn}}{\omega_{mn}} \quad (\text{F19})$$

defines the quantity

$$\chi_m^\lambda = \sum_{\substack{n \in \text{filled} \\ m \in \text{empty}}} \frac{\Omega_\lambda^{mn}}{\omega_{mn}}. \quad (\text{F20})$$

Appendix G: Bounds on Sum Rules

Following ref. [67], we consider a function of generalized sum rules of longitudinal conductivity (which is positive definite)

$$h(\beta) = \int_0^\infty \frac{\text{Re}[\sigma_{L,\mu}(\omega)]}{\omega} (\omega^m + \beta\omega^n)^2 \quad (\text{G1})$$

which can be written as

$$h(\beta) = S_{2m} + 2\beta S_{m+n} + \beta^2 S_{2n} \quad (\text{G2})$$

where we have used the shorthand $S_m = S_{L,\mu}^m$ for the longitudinal sum rule. Since $\text{Re}[\sigma_{L,\mu}(\omega)] \geq 0$, and the limits of the integral are from 0 to ∞ , the function h is positive semi-definite. It implies that the minimum of h is positive semi-definite as well. Finding the minima gives the condition

$$h'(\beta^*) = 0, \quad \beta^* = -\frac{S_{m+n}}{S_{2n}}, \quad h(\beta^*) = S_{2m} - \frac{S_{m+n}^2}{S_{2n}} \geq 0 \quad (\text{G3})$$

and hence we get the relation

$$S_{m+n}^2 \leq S_{2m} S_{2n} \quad (\text{G4})$$

which is valid for any $m, n \in \mathbb{R}$.

Appendix H: Tight-Binding Models

For completeness, we enumerate the details of various tight-binding models used in the main text.

1. Honeycomb Lattice with Inversion Breaking Mass Term

We consider a honeycomb lattice with two inequivalent sites A and B . With one orbital at each site, the lattice is described by the lattice vectors and basis

$$\mathbf{a}_1 = (\sqrt{3}/2, 1/2), \quad \mathbf{a}_2 = (\sqrt{3}/2, -1/2), \quad \boldsymbol{\tau} = \frac{1}{3}(\mathbf{a}_1 + \mathbf{a}_2) \quad (\text{H1})$$

with $\tau_A = \mathbf{0}$ and $\tau_B = \boldsymbol{\tau}$. The Bloch Hamiltonian for nearest neighbor hopping and inversion breaking mass is given by

$$\mathcal{H} = \int_{\text{BZ}} d\mathbf{k} \begin{pmatrix} c_{A,\mathbf{k}}^\dagger & c_{B,\mathbf{k}}^\dagger \end{pmatrix} \begin{pmatrix} m_z & \gamma(\mathbf{k}) \\ \gamma(\mathbf{k})^* & -m_z \end{pmatrix} \begin{pmatrix} c_{A,\mathbf{k}} \\ c_{B,\mathbf{k}} \end{pmatrix} \quad (\text{H2})$$

where

$$\gamma(\mathbf{k}) = \sum_{j=1}^3 e^{i\mathbf{k}\cdot\boldsymbol{\delta}_j}, \quad \boldsymbol{\delta}_j = R_z(2\pi j/3)\boldsymbol{\tau}. \quad (\text{H3})$$

$R_z(\theta)$ here denotes a rotation matrix about the \hat{z} axis by angle θ . The resulting band structure has two bands with the minimum gap given by $\hbar\omega_g = 2m_z$.

2. Haldane Model for Chern Insulator

Haldane model includes both nearest neighbor hopping and inversion breaking mass as described in the previous section, in addition to a next-nearest neighbor hopping with a flux [79]. The Bloch Hamiltonian is given by

$$\mathcal{H} = \int_{\text{BZ}} d\mathbf{k} \begin{pmatrix} c_{A,\mathbf{k}}^\dagger & c_{B,\mathbf{k}}^\dagger \end{pmatrix} \begin{pmatrix} m_z + t_2\Gamma(\phi, \mathbf{k}) & t\gamma(\mathbf{k}) \\ t\gamma(\mathbf{k})^* & -m_z + t_2\Gamma(-\phi, \mathbf{k}) \end{pmatrix} \begin{pmatrix} c_{A,\mathbf{k}} \\ c_{B,\mathbf{k}} \end{pmatrix} \quad (\text{H4})$$

where

$$\Gamma(\phi, \mathbf{k}) = 2 \sum_{j=1}^3 \cos(\mathbf{k} \cdot \mathbf{A}_j + \phi), \quad \mathbf{A}_j = R_z(2\pi j/3) \mathbf{a}_1. \quad (\text{H5})$$

The model has two bands with gap $m_z \pm 3\sqrt{3}t_2 \sin(\phi)$ at the two valleys $\pm \mathbf{K}$. The system undergoes a topological phase transition at $m_z = 3\sqrt{3}t_2 \sin(\phi)$. For $\phi = \pi/2$, this corresponds to $m_z \approx 5.2t_2$.

3. Lieb Lattice to Square Lattice Model

We consider a four-orbital tight-binding model with lattice vectors

$$\mathbf{a}_1 = (1, 0), \quad \mathbf{a}_2 = (0, 1), \quad \boldsymbol{\tau}_A = \mathbf{0}, \quad \boldsymbol{\tau}_B = \mathbf{a}_1/2, \quad \boldsymbol{\tau}_C = \mathbf{a}_2/2, \quad \boldsymbol{\tau}_D = \mathbf{a}_1/2 + \mathbf{a}_2/2 \quad (\text{H6})$$

given by the Bloch Hamiltonian

$$\mathcal{H} = \int_{\text{BZ}} d\mathbf{k} \begin{pmatrix} c_{A,\mathbf{k}}^\dagger & c_{B,\mathbf{k}}^\dagger & c_{C,\mathbf{k}}^\dagger & c_{D,\mathbf{k}}^\dagger \end{pmatrix} \begin{pmatrix} 0 & tg_x & tg_y & 0 \\ tg_x & 0 & 0 & t_p g_y \\ tg_y & 0 & 0 & t_p g_x \\ 0 & t_p g_y & t_p g_x & 0 \end{pmatrix} \begin{pmatrix} c_{A,\mathbf{k}} \\ c_{B,\mathbf{k}} \\ c_{C,\mathbf{k}} \\ c_{D,\mathbf{k}} \end{pmatrix} \quad (\text{H7})$$

where the function g is defined as

$$g_x = -2 \cos(\mathbf{k} \cdot \mathbf{a}_1/2), \quad g_y = -2 \cos(\mathbf{k} \cdot \mathbf{a}_2/2). \quad (\text{H8})$$

When $t_p = t$, the model is identical to a square lattice, expressed in a larger unit cell. With $t_p = 0$, the D orbital factors out and the resulting lattice is the Lieb lattice with an exact flat band at zero energy.